Spin Dynamics Simulation of the Z2-vortex Fluctuations

Mizuta, Yo P.

Aoyama, Kazushi

Tomiyasu, Keisuke

Matsuura, Masato

Kawamura, Hikaru

Spin Dynamics Simulation of the Z_2-vortex Fluctuations

Yo P. Mizuta[1], Kazushi Aoyama[2], Keisuke Tomiyasu[3],
Masato Matsuura[4], and Hikaru Kawamura[5]*

[1]*Graduate School of Engineering Science, Osaka University, Toyonaka, Osaka 560-8531, Japan*
[2]*Department of Earth and Space Science, Graduate School of Science, Osaka University, Toyonaka, Osaka 560-0043, Japan*
[3]*Nissan ARC Ltd., Yokosuka, Kanagawa 237-0061, Japan*
[4]*CROSS Neutron Science and Technology Center, IQBRC Bldg, Tokai, Ibaraki 319-1106, Japan*
[5]*Molecular Photoscience Research Center, Kobe University, Kobe 657-8501, Japan*

Motivated by the recent quasi-elastic neutron scattering experiment, we extend the spin-dynamics simulation on the triangular-lattice Heisenberg antiferromagnet, to observe a sharp central peak of its energy width ~0.001J (J the exchange coupling) of the Z_2-vortex origin, consistently with the experiment.

Some time ago, Kawamura and Miyashita pointed out that the frustrated isotropic Heisenberg magnets in two dimensions could possess a novel vortex characterized by the parity-like two-valued topological number corresponding only to its presence/absence, a Z_2 vortex, which drove a topological transition at a finite temperature $T = T_V$ associated with its binding-unbinding.[1] Interestingly, the spin correlation length stays finite even at and below T_V, and the low-T phase is the spin paramagnetic state with topologically broken ergodicity, called the spin-gel state.[2,3]

While the direct experimental observation of the Z_2 vortex has remained elusive for years, a very recent quasi-elastic neutron scattering (QENS) experiment performed on the powder sample of the quasi-two-dimensional (2D) triangular-lattice Heisenberg antiferromagnet NaCrO$_2$ has succeeded in directly probing the signature of the free Z_2 vortex via the observation of a sharp quasi-elastic (QE) scattering of its energy width as narrow as ~10 μeV corresponding to ~0.001J (J the exchange coupling) in the finite-T range of 30–40 K.[4] As this material has been considered to be a promising candidate of the Z_2-vortex-bearing system,[5] it seems fully consistent to identify the origin of the observed sharp QE scattering as the dynamics of the free Z_2 vortex.

The theoretical proposal that the signature of the free Z_2 vortex might be detectable via the appearance of a sharp central peak (QE scattering) in the dynamical spin structure factor at $T \gtrsim T_V$ was made earlier.[6] Indeed, by the spin-dynamics simulation on the triangular-lattice Heisenberg model with the nearest-neighbor (nn) antiferromagnetic (AF) coupling J, the appearance of such Z_2-vortex-induced central peak of the width ~0.01J at $T > T_V \simeq 0.285J$ was numerically obtained.[6] The central-peak width in the recent experiment on NaCrO$_2$, however, was even narrower than that in the model simulation[6] by an order of magnitude. One might wonder if it might be possible to numerically reproduce an order-of-magnitude sharper central peak as observed in the recent experiment.[4]

In order to examine this issue, we extend the earlier simulation of Ref. 6 to longer simulation time and to larger lattices. Longer simulation time is implemented to improve the ω-resolution required to detect the sharp structure as a function of ω, and we implement here twenty times longer simulation time than that of Ref. 6. Larger lattice sizes enable us to deal with more isolated, long-lived free Z_2 vortex, and we treat here the lattices of its linear size twice as large as that treated in Ref. 6.

The model considered is the same as that in Ref. 6, i.e., the AF classical Heisenberg model on the 2D triangular lattice, whose Hamiltonian is given by $\mathcal{H} = J \sum_{i,j} S_i \cdot S_j$ ($J > 0$), where the sum is taken over all nn pairs on the $L \times L$ triangular lattice under periodic boundary conditions. We set here $L = 768$ and 1536.

Following Ref. 6, the spin dynamics simulation is performed according to the classical analogue of the Bloch equation [see Eq. (3) of Ref. 6]. The temperature effect is taken into account via the initial spin configurations generated by the equilibrium Monte Carlo (MC) simulation at temperature T based on the combined heat-bath and over-relaxation methods. The time evolution of the spins is solved by the fourth-order Runge–Kutta method, where the time mesh Δt is taken to be 0.01 (in the unit of $\hbar/J$), commonly with Ref. 6. The maximum simulation time t_{max} is taken to be 16,000, twenty times longer than t_{max} of Ref. 6. Thermal average is taken by averaging over 200–1000 independent runs with different spin initial conditions.

We compute the dynamical spin structure factor,

$$S(\boldsymbol{q}, \omega) = \langle |\boldsymbol{S}_{\boldsymbol{q}}(\omega)|^2 \rangle, \tag{1}$$

$$\boldsymbol{S}_{\boldsymbol{q}}(\omega) = \int dt \sum_i \boldsymbol{S}_i(t) \exp[-i(\boldsymbol{q} \cdot \boldsymbol{r}_i + \omega t)], \tag{2}$$

where $\boldsymbol{q}$ is the wavevector, ω the angular frequency, and $\langle \cdots \rangle$ denotes the thermal average.

Typical ω-dependence of the computed $S(\boldsymbol{q}, \omega)$ close to the K point is shown in Fig. 1(a), where the temperature $T/J = 0.295$ is slightly above $T_V/J = 0.285$ and the wave vector $\boldsymbol{q}$ is slightly away from the K point in the direction of the M point with $|\boldsymbol{q} - \boldsymbol{q}_K| = \frac{2\pi}{192}$ (in the unit of $\frac{1}{a}$, a being the lattice constant). As can be seen from Fig. 1(a), a central peak is observed in addition to the side peak originating from the damped spin waves. The data are collected for various temperatures and wavevectors lying on the line connecting the K and M points, and are fitted by the form,

$$C_L \frac{1}{\omega^2 + \Gamma_L^2} + C_{DHO} \frac{\omega_0^2 \Gamma}{(\omega^2 - \omega_0^2)^2 + \Gamma^2 \omega^2} + C_0, \tag{3}$$

where the first Lorentzian term represents the QE central peak of the amplitude C_L and the width Γ_L, the second term the contribution of the damped harmonic oscillator (DHO) of the frequency ω_0, the width Γ and the amplitude C_{DHO}, the last term being the constant background. We show in Fig. 1(a) the fitting results of the raw $S(\boldsymbol{q}, \omega)$ data where the best fitted curve is shown together with the contribution of the three terms in Eq. (3). Reasonably good fit is obtained.

Figures 1(b) and 1(c) exhibit the width Γ_L (b) and the integrated intensity (c) of the QE central peak plotted versus the wavevector $|\boldsymbol{q} - \boldsymbol{q}_K|$ for several temperatures around T_V. As can be seen from Fig. 1(b), the width Γ_L gets narrower as T approaches T_V from above, and as $\boldsymbol{q}$ approaches $\boldsymbol{q}_K$. In
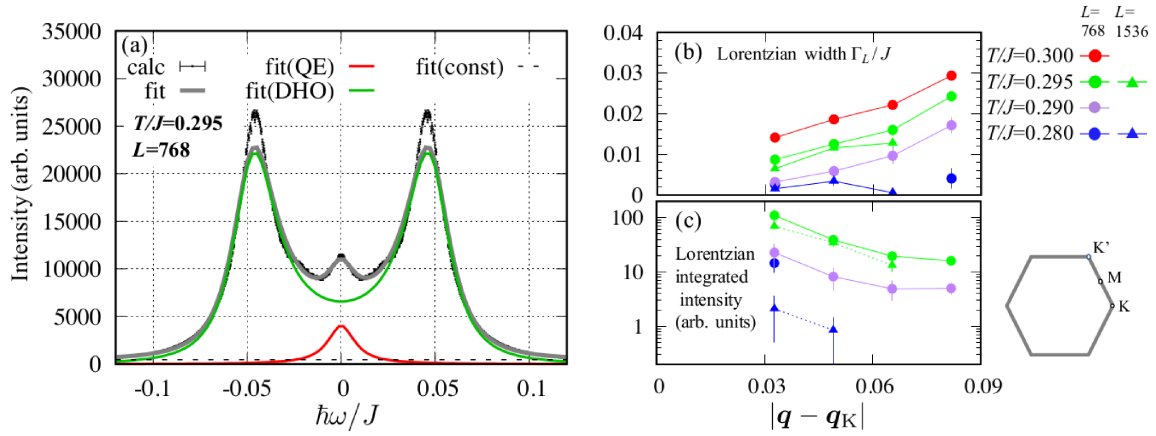
Fig. 1. (Color online) (a) The ω dependence of $S(\boldsymbol{q},\omega)$ computed at a temperature $T/J = 0.295$ just above $T_V/J = 0.285$, and at the wavevector $\boldsymbol{q} = \boldsymbol{q}_K + \frac{1}{64}(\boldsymbol{q}_K - \boldsymbol{q}_M)$ close to the K-point for the size $L = 768$. The best fitted curve based on Eq. (3) is also shown, together with the contribution of each term, i.e., the QE central peak, the DHO term, and the constant (const) term. (b) The energy width and (c) the integrated intensity of the fitted QE central peak plotted versus the distance from the K point along the KM line, $|\boldsymbol{q} - \boldsymbol{q}_K|$ in the unit of $\frac{1}{a}$, illustrated in the hexagon representing the 1st Brillouin zone shown at the right bottom.

particular, Γ_L gets as small as $\sim 0.001J$ just above T_V in the close vicinity of the K point. The earlier estimate $\sim 0.01J$ was obtained at $|\boldsymbol{q} - \boldsymbol{q}_K| = \frac{4\pi}{192}$ with the lower ω-resolution,[6] but is numerically consistent with our present result. Theoretically, Γ_L is expected to get further smaller than $\sim 0.001J$ as $T \to T_V$ and $\boldsymbol{q} \to \boldsymbol{q}_K$ for large enough L, while the experimental detection of the QENS of the width narrower than $\sim 0.001J$ would presently be difficult due to the current ω-resolution limit of the detector. One can also see from Fig. 1(c) that the QE central-peak intensity tends to decrease as T approaches T_V, eventually vanishing at $T < T_V$, while it gets larger as $\boldsymbol{q}$ approaches $\boldsymbol{q}_K$. It was already pointed out in Ref. 6 that the width of the QE central peak is quite narrow in the vicinity of the K point and is much broader far away from the K point, where the former was associated with the free Z_2 vortices, while the latter associated with the bound Z_2-vortex pairs. Our present observation, which reveals the systematic variation of the width against $\boldsymbol{q}$, is fully consistent with such a previously proposed picture.

On the basis of our present observation, we wish to discuss experimental implications. As the recent QENS measurements on $NaCrO_2$ were performed on the powder sample, the measured intensity is not the contribution from a single particular $\boldsymbol{q}$, but rather the average over the contributions from various $\boldsymbol{q}$'s. Our result suggests that, through the powder averaging over various $\boldsymbol{q}$'s, the resulting QE scattering intensity would become a superposition of many Lorentzians with continuously distributed widths. Since the free Z_2 vortex near T_V yields the central peak of the narrowest width of $\sim 0.001J$ with a significant intensity among nearby $\boldsymbol{q}$'s, it would be visible even after the powder average. Indeed, the recent QENS experiment succeeded in

clearly catching the corresponding sharp QE scattering of its width $0.01\,\mathrm{meV} \sim 0.001J$.[4]

We note that, in the analysis of Ref. 4, the superpositions of these continuously distributed Lorentzians are approximated by the three Lorentzians, i.e., very sharp L_1-component of $\sim 0.01\,\mathrm{meV}$ width describing the free Z_2 vortex, L_2-component of $\sim 0.1\,\mathrm{meV}$ width describing the typical Z_2-vortex pairs, and L_3-component of $\sim 1\,\mathrm{meV}$ width describing the damped spin waves. The analysis, though an approximation, is expected to capture the essential part of relevant fluctuations. Our present analysis then suggests that the L_1-component is borne by the contributions close to the K-point, while the L_2-component borne by those away from the K-point. Meanwhile, if the QENS experiment could be performed on single crystal, more detailed information including the $\boldsymbol{q}$ dependence might be obtained, which would make further detailed comparison with the theory possible. Thus, single-crystal QENS measurements on the Z_2-vortex-bearing magnet remain to be an interesting future task.

*h.kawamura.handai@gmail.com
1) H. Kawamura and S. Miyashita, J. Phys. Soc. Jpn. **53**, 4138 (1984).
2) H. Kawamura, A. Yamamoto, and T. Okubo, J. Phys. Soc. Jpn. **79**, 023701 (2010).
3) H. Kawamura, J. Phys.: Conf. Ser. **320**, 012002 (2011).
4) K. Tomiyasu, Y. P. Mizuta, M. Matsuura, K. Aoyaman, and H. Kawamura, arXiv:2110.15068.
5) A. Olariu, P. Mendelse, F. Bert, B. G. Ueland, P. Schiffer, R. F. Berger, and R. J. Cava, Phys. Rev. Lett. **97**, 167203 (2006).
6) T. Okubo and H. Kawamura, J. Phys. Soc. Jpn. **79**, 084706 (2010).